Electrodeposition of ZnO Nanostructures: Growth, Doping, and Physical Properties

19

M. Allan Thomas and Jingbiao Cui

Contents

Abstract

ZnO is one of the most promising semiconductors for low-cost optoelectronics and can be obtained from a variety of deposition techniques. Among them, electrochemical growth in aqueous solution has become an important approach for ZnO deposition with abundant morphologies and doping capabilities. This chapter summarizes the current achievements in electrodeposition of ZnO and also

M.A. Thomas (✉)
Department of Physics and Astronomy, University of Arkansas at Little Rock, Little Rock, AR, USA
e-mail: mathomas1@ualr.edu

J. Cui
Department of Physics, University of Memphis, Memphis, TN, USA
e-mail: jcui@memphis.edu

M. Aliofkhazraei, A.S.H. Makhlouf (eds.), *Handbook of Nanoelectrochemistry*,
DOI 10.1007/978-3-319-15266-0_22

discusses the challenges and extensive potential in this research area. The effects of electrochemical growth conditions, annealing, and doping on the structural, optical, and electrical properties of ZnO thin films and nanowires are presented in detail. Electrical characterization using electrochemical impedance spectroscopy and photoelectrochemical cell measurements are also included. *n*-Type and *p*-type semiconductor nanowires are achieved by electrochemical doping of ZnO with various elements such as Cl and Ag and are discussed as nanoscale building blocks in advanced optoelectronics. Electrochemical deposition of highly uniform ZnO thin films and oriented ZnO nanowire arrays with desired physical properties opens up possibilities for large-scale and economic fabrication of advanced optoelectronic devices.

Keywords
ZnO • Electrodeposition • Doping • Optoelectronics • Nanomaterials

Introduction

ZnO Basics

ZnO is a semiconductor with a direct bandgap of 3.37 eV (368 nm) at room temperature. ZnO is therefore transparent to visible light, yet still a semiconductor. Such a combination of properties is rare and enables ZnO to be considered for a much wider span of device applications. ZnO also possesses an exciton binding energy of 60 meV [1], which is significantly larger than its comparable materials GaN (25 meV) and ZnSe (22 meV). Excitonic processes in ZnO, such as those associated with light-emitting diode (LED), laser diode, and solar cell operation, will be significantly more efficient and effective as compared to other wide bandgap semiconductors. Optical processes involving excitons in ZnO also produce a rich variety of interesting physics and behavior, making ZnO an attractive material not only for devices but also for fundamental research.

Growth Techniques

The available growth techniques for ZnO are practically endless. Nearly every deposition method for materials has been exploited to obtain ZnO in bulk, thin film, or nanostructure form [2]. Many of the common growth techniques for ZnO are associated with relatively high temperatures and vacuum environments, such as molecular beam epitaxy (MBE) [3], chemical vapor deposition (CVD) [4], pulsed laser deposition (PLD) [5, 6], thermal evaporation [7], and sputtering [8]. Bulk ZnO single crystals can be formed in hydrothermal [9], chemical vapor transport [10], and pressurized melt-growth processes [11]. ZnO materials from these high-temperature growth methods are often of very high quality and serve as the stepping stone for

ZnO's breakthrough into the device application market. But perhaps the most interesting distinction for ZnO among other semiconductors is its amenability to be deposited at low growth temperatures (<200 °C) and in aqueous solution.

Electrochemical Growth in Aqueous Solution

The device application potential of ZnO in the areas of electronics and optoelectronics relies on achieving large-scale and homogeneous materials at low cost as well as controlling ZnO's fundamental physical properties. As mentioned above, a wide variety of growth techniques has been explored to accomplish these goals and obtain ZnO materials for potential use in device applications. In particular, low-temperature growth processes for ZnO materials are becoming increasingly studied due to their low cost and scale-up potential [12, 13]. Solution-based techniques for depositing ZnO include electrochemical deposition (ECD), hydrothermal and/or chemical bath deposition methods, sol–gel processes, and spray pyrolysis, just to name a few. For a thorough and enlightening review of solution-based techniques for ZnO deposition, see Ref. [12]. The various growth techniques and materials that can be deposited for ZnO are summarized in Table 1.

This chapter is focused on ECD growth processes for ZnO, and therefore they receive most of the attention here. The current achievements, challenges, and extensive potential in the area of ZnO ECD are summarized. The effects of electrochemical growth conditions, annealing, and doping on the structural, optical, and electrical properties of ZnO nanowires and thin films are presented in detail. Recent work on utilizing ECD ZnO nanowires as nanoscale building blocks for advanced

Table 1 Growth techniques and materials available for ZnO

ZnO materials and growth methods			
High temperature (>100 °C)			
Method	Environment	Structure types	References
MBE	High vacuum	Thin films, 3D nano	[3]
CVD	Moderate vacuum	Thin films, 3D nano	[4]
PLD	High vacuum	Thin films, 3D nano	[5, 6]
Evaporation	High vacuum	Thin films	[7]
Sputtering	High vacuum	Thin films, 3D nano	[8]
Hydrothermal	Ionic solution	Single crystal	[9]
CVT	Moderate vacuum	Single crystal	[10]
PMG	High pressure	Single crystal	[11]
Low temperature (<100 °C)			
CBD	Aqueous	Thin films, 3D nano	[12, 13, 21–24]
ECD	Aqueous	Thin films, 3D nano	[12, 14, 15, 25]

Abbreviations: *MBE* molecular beam epitaxy, *CVD* chemical vapor deposition, *PLD* pulsed laser deposition, *CVT* chemical vapor transport, *PMG* pressurized melt growth, *CBD* chemical bath deposition, *ECD* electrochemical deposition, *Nano* nanostructures

optoelectronic devices is also highlighted. ECD of highly uniform ZnO thin films and oriented ZnO nanowire arrays with desired physical properties opens up possibilities for large-scale and economic fabrication of advanced optoelectronic devices.

ECD ZnO: Methods, Materials, and Properties

Electrochemical Growth of ZnO: A History

In 1996, two alternative methods for ECD of ZnO were introduced: (1) the dissolved oxygen method developed by Peulon and Lincot [14] and (2) the zinc nitrate method developed by Izaki and Omi [15]. The amount of research activity associated with similar low-cost and low-temperature growth methods for ZnO materials has increased tremendously since then. The basic scheme to produce ZnO in ECD processes is as follows:

$$\text{Ion species} + e^- \rightarrow OH^- \tag{1}$$

$$Zn^{2+} + 2OH^- \rightarrow Zn(OH)_2 \tag{2}$$

$$Zn(OH)_2 \rightarrow ZnO + H_2O \tag{3}$$

$$Zn^{2+} + 2OH^- \rightarrow ZnO + H_2O \tag{4}$$

The first requirement is the production of hydroxide ions (OH^-) in the growth solution, and typically this step is accomplished by an electrochemical reduction reaction (Eq. 1). In the zinc nitrate method, the ion species in Eq. 1 is NO_3^-, while in the dissolved oxygen method, it is O_2 gas bubbled into the growth solution. Once produced, the OH^- ions react with zinc ions (Zn^{2+}) also present in the solution to eventually form ZnO. Zn^{2+} ions are already present in the zinc nitrate method, but in the dissolved oxygen method, they must come from a secondary source such as zinc chloride, perchlorate, acetate, or sulfate. Many studies of solution-based processes in the literature list Eqs. 2 and 3 as the eventual pathway for ZnO crystallization, which involves an intermediary $Zn(OH)_2$ phase [12, 16, 17]. However, recent investigations have provided strong support for the idea that Eq. 4 is the route for ZnO formation – a direct crystallization from Zn^{2+} and OH^- ions that does not involve any intermediate hydroxide phase [18]. If $Zn(OH)_2$ is an intermediate to eventual ZnO formation, only under appropriate conditions of pH, temperature, and concentrations will it decompose to produce ZnO and water (Eq. 3) [12].

Among the various options for ECD ZnO, there is not a single method that possesses all of the desirable traits for ease of use and process flexibility. While the zinc nitrate method is likely the simplest in that only one source material is needed and it is not necessary to make dissolved oxygen solutions, it possesses the smallest ZnO (instead of Zn) deposition potential window due to the reduction potential of

the nitrate reduction reaction [15]. Meanwhile, both the dissolved oxygen and hydrogen peroxide processes [19, 20] require a secondary source material to obtain Zn^{2+} ions, creating an immediate situation of unwanted and potentially contaminant species in the growth solution. Regarding the viability of process scalability, in principle only the dissolved oxygen method is limited due to the low solubility of O_2 gas in water which creates an upper boundary on the growth rate of ZnO materials by this method.

In addition to ECD, there are many similar techniques for depositing ZnO materials in solution. Another low-temperature deposition method for ZnO materials that has experienced a seemingly exponential increase in growth since its beginnings in 2001 [12] is the so-called hydrothermal or chemical bath deposition [21–24]. This method is actually quite similar to ECD of ZnO in aqueous solution in that chemical species are mixed in water and a reaction between Zn^{2+} and OH^- ions eventually produces ZnO [12]. Only substrates with specific properties and of certain materials can be utilized in the hydrothermal growth processes, however, due to limited initial ZnO nucleation.

Based on the difficulty in facilitating ZnO nucleation in chemical bath deposition and hydrothermal processes [21–24], Cui and Gibson developed a new ECD method for ZnO in 2005 which is a modified version of the most common hydrothermal growth process (zinc nitrate and hexamine, [21]) [25]. This method exploits the benefits and overcomes the limitations of both the zinc nitrate ECD process and the zinc nitrate plus hexamine hydrothermal process by combining them together. By applying a potential during growth, it becomes possible to significantly increase the nucleation density and growth rate of ZnO as compared to strictly hydrothermal processes. This allows for the deposition of ZnO directly onto conducting or semiconducting substrates (e.g., polished Si) without the need for a ZnO seed layer. In addition, the electrochemical growth of ZnO in a solution that contains zinc nitrate as well as hexamine immediately provides the ability to obtain controlled 3D nanowire structures [25]. While both the zinc nitrate and dissolved oxygen ECD methods for ZnO were initially developed for thin film deposition, work on both processes over the years has enabled modifications, such as the zinc nitrate plus hexamine method [25], that allow for significant tunability of the ZnO structures to include 3D nanowires and other useful morphologies. The growth conditions and structural properties for a wide range of ECD ZnO materials and methods are summarized in Table 2 and then discussed at length and in detail below.

ECD ZnO: Dissolved Oxygen Method

Much like any other deposition method for ZnO, the specific growth conditions in the ECD process maintain a strong effect on the eventual physical properties of the materials. Since all ECD methods for depositing ZnO eventually involve the reaction of Zn^{2+} ions with OH^- ions to make ZnO, the relative concentration of these two species near the electrode/growing crystal surface is expected to play a dominant role in governing the properties of the ZnO materials obtained. Even though the

Table 2 Growth conditions and structural properties for ECD ZnO materials

ECD ZnO: growth conditions and structural properties			
Dissolved oxygen method			
Main conditions	Substrate/special condition	Structural	References
0.5 mM [Zn^{2+}], 0.1 M KCl	FTO	Nanowires	[14, 26]
5 mM [Zn^{2+}], 0.1 M KCl	FTO	Dense films	[14, 27]
0.5 mM [Zn^{2+}], 0.1 M KCl	FTO; Cl^-, SO_4^-, acetate ions added	Nanowires (various aspect ratios)	[29]
Zinc nitrate method			
[$Zn(NO_3)_2$]	Substrate/special condition	Structural	References
0.1 M	ITO; low potential	3D nano	[15]
0.1 M	ITO; high potential	Dense films	[15]
8–10 mM	Si, poly Au, ITO; hexamine added	Nanowires	[25]
0.5–3 mM	ITO	Nanowires	[29]
0.05 M	Poly Au; galvanostatic, low current	Dense films	[31]
0.05 M	Poly Au; galvanostatic, high current	Nanowires	[31]
0.05–0.1 mM	ZnO seed; [NO_3^-] source: 0.1 M $NaNO_3$	Nanowires (various aspect ratios)	[35]
0.05 M	Poly Au	Nanowires	[36]
0.05 M	Poly Au; 30–70 % methanol electrolyte	Dense films	[36, 41]
0.05 M	Poly Au; 70–100 % methanol electrolyte	Nanosheets, nanowalls	[41]
0.08 M	ITO; 25 % ethanol electrolyte	Dense films	[37]

Abbreviations: *FTO* fluorine-doped tin oxide, *ITO* indium tin oxide, *Nano* nanostructures, *poly* polycrystalline

eventual ZnO formation mechanism is the same in all ECD ZnO processes, many factors related to the particular ECD method and growth conditions used will affect the [Zn^{2+}]/[OH^-] ratio.

In the dissolved oxygen method, precursor concentration limits are very much set by the low solubility of O_2 gas in solution. As a result, the concentrations of the reactant species used to deposit ZnO are typically very low, and a supporting electrolyte such as KCl or $KClO_4$ is used to establish a growth solution conductivity that is amenable to ECD processes. The initial [Zn^{2+}] and [O_2] are quite small, even below the mM range [14, 26], resulting in a strong effect of [Zn^{2+}] as it is increased to higher concentrations. At low zinc concentrations, e.g., 0.5 mM, 3D nanowire-type structures can be deposited (Fig. 1) [14, 26], while at slightly higher [Zn^{2+}], such as 5 mM, more dense and 2D type thin film structures are obtained (Fig. 2) [14, 27]. An even finer tuning of [Zn^{2+}] in the 3D nanowire regime enables control of the nanowire diameter from 25 to 80 nm [28].

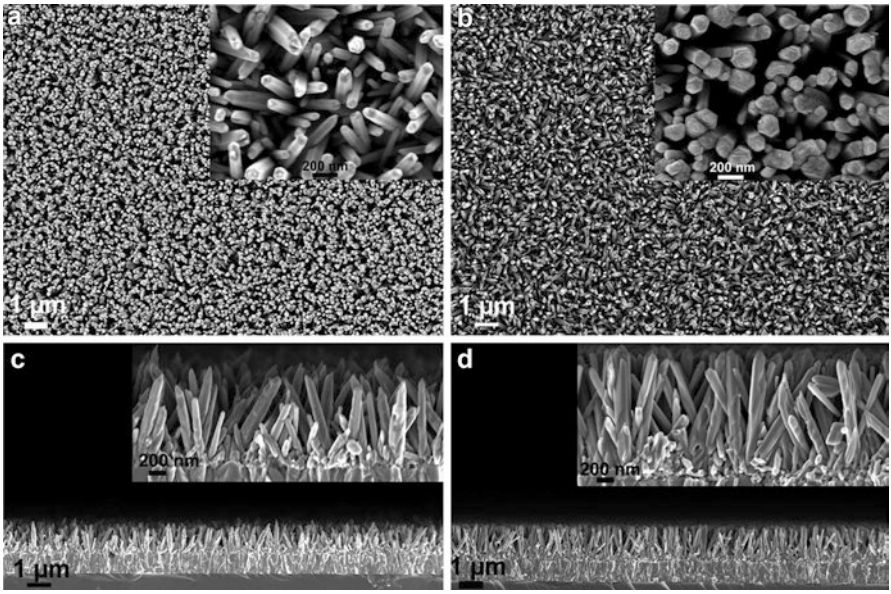

Fig. 1 SEM images of 3D ZnO nanowires obtained from the dissolved oxygen method with $[Zn^{2+}]=0.5$ mM (Reproduced with permission from Tena-Zaera et al. [26]. Copyright (2008) American Chemical Society)

Other chemical species can be used to modify the ZnO growth process in the dissolved oxygen ECD method. Various additives such as Cl^-, acetate, and SO_4^{2-} can control the ZnO nanowire aspect ratio [29]. While additional Cl^- leads to thicker and shorter nanowires, i.e., a low aspect ratio (Fig. 3a, b), acetate ions enable the growth of longer and thinner nanowires to significantly increase their aspect ratio (Fig. 3e, f). Cyclic voltammetry (CV) studies indicate the various ion species preferentially adsorb onto the growing ZnO crystal surface in different ways and also affect the electrochemical reduction of O_2 [29]. Both of these factors change the local ZnO growth environment and in turn modify the rate and type of ZnO deposition.

ECD ZnO: Zinc Nitrate Method

While the zinc nitrate ECD method utilizes a similar reaction pathway for depositing ZnO, it is certainly distinct from the dissolved oxygen process in several ways. Perhaps most importantly, zinc nitrate is the only necessary precursor material – it serves as the Zn^{2+} source and the OH^- source (via reduction of nitrate). Furthermore, zinc nitrate is highly soluble in water; therefore, much larger precursor concentrations can be used. This situation is quite different from the dissolved oxygen method, suggesting that ECD of ZnO with the zinc nitrate method will lead to unique

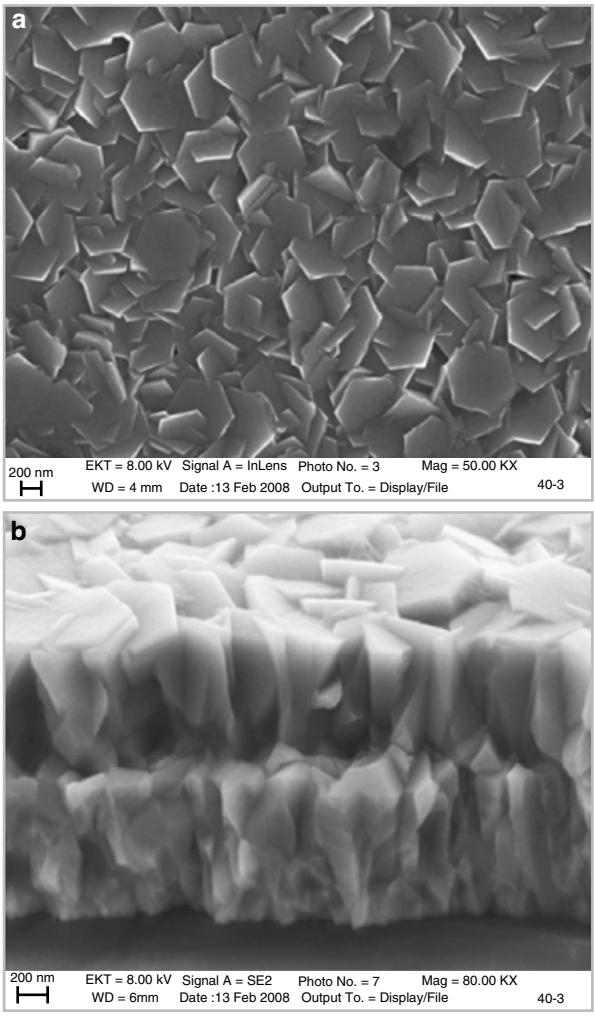

Fig. 2 SEM images of 2D ZnO thin films obtained from the dissolved oxygen method with $[Zn^{2+}] = 5$ mM (Adapted with permission from Rousset et al. [27]. Copyright (2009) American Chemical Society)

conditions for crystal growth and in turn physical properties of the ZnO materials are obtained. Various growth conditions such as $[Zn^{2+}]$, $[NO_3^-]$, temperature, applied potential, and electrolyte additives in the zinc nitrate method have been tested thoroughly in the literature.

Growth Conditions and Structural Properties

In the original work on the zinc nitrate ECD method, it was shown that the applied potential during growth affects the structural properties of the ZnO materials significantly [15]. More defined and 3D-type structures are formed at lower potentials

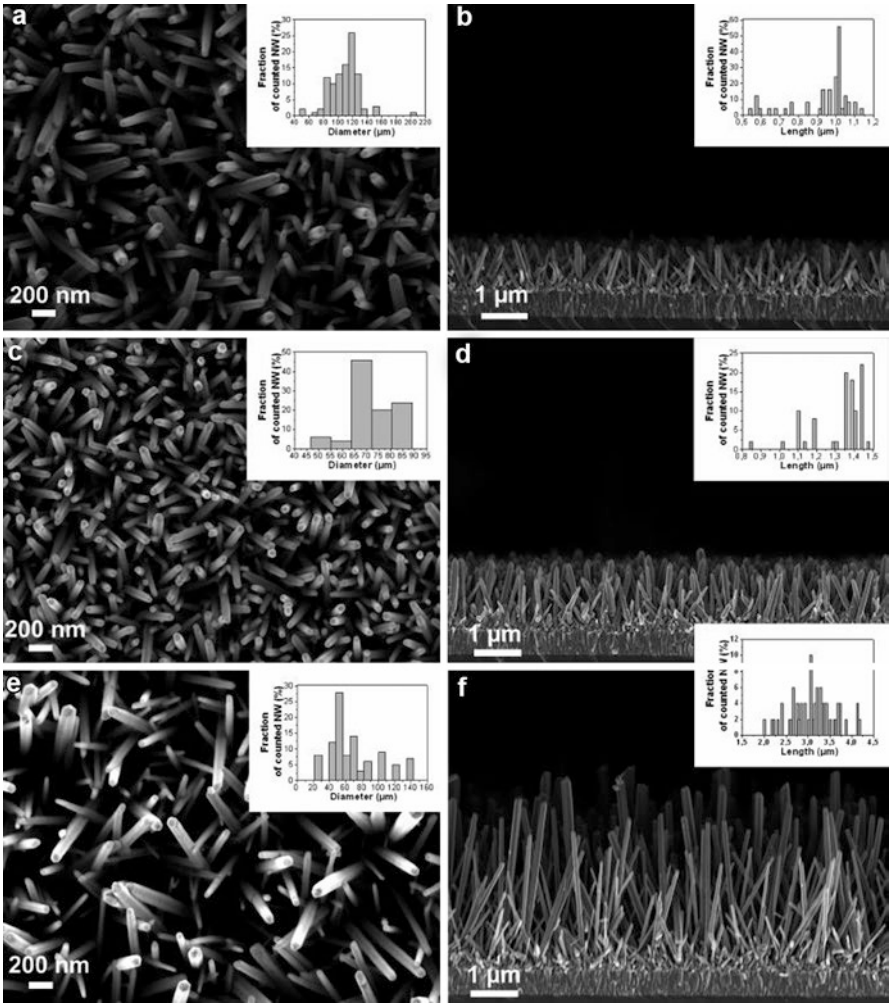

Fig. 3 SEM images of ZnO nanowires from the dissolved oxygen method with the addition of (**a**, **b**) Cl^-, (**c**, **d**) SO_4^{2-}, and (**e**, **f**) acetate ions. Diameter and length distributions are shown in the insets of each figure (Reproduced with permission from Elias et al. [29]. Copyright (2008) American Chemical Society)

(near the limit for reduction of nitrate to occur), while more dense and 2D film structures are obtained at more negative potentials well into the overpotential regime (Fig. 4). As expected, the ZnO growth rate is also strongly affected by the growth potential with a significant increase for more negative potentials [15].

More recent work associated with growth conditions in the zinc nitrate ECD method showed that, much like in the dissolved oxygen process, a lower $[Zn^{2+}]$ during growth leads to truly 3D nanowire structures [30]. In the same work, the authors also concluded that an increased negative growth potential in fact leads to denser and more

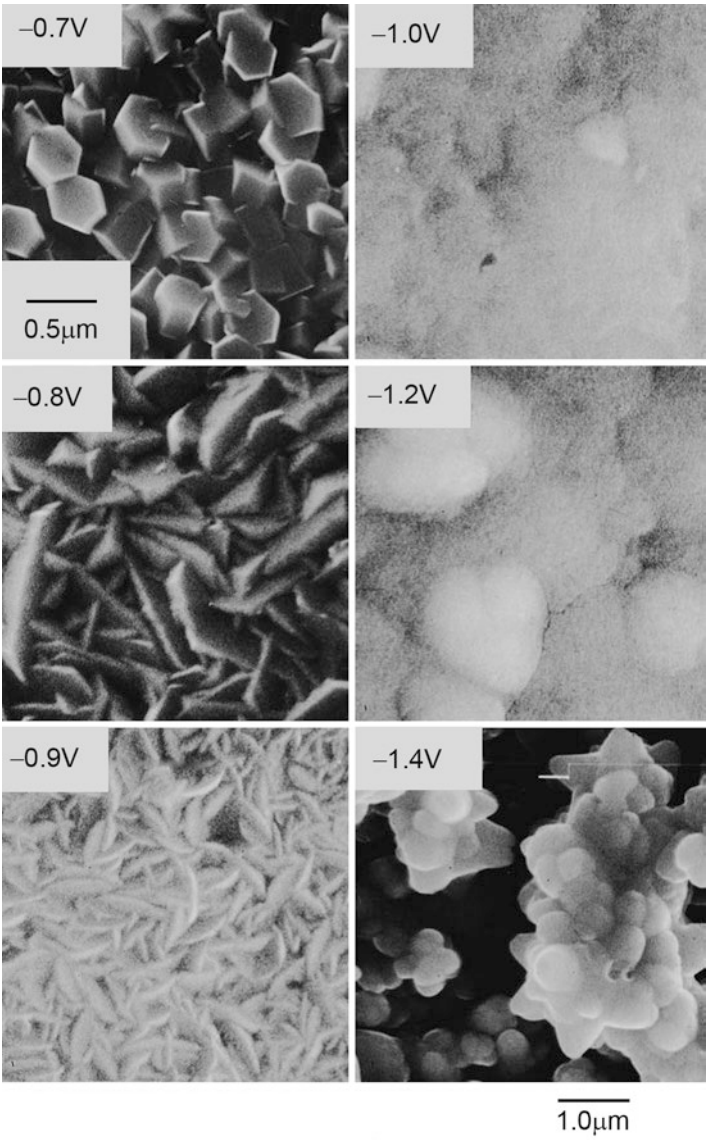

Fig. 4 SEM images of ZnO materials obtained by the zinc nitrate method. The applied potentials as measured relative to an Ag/AgCl reference electrode are shown in the figures (Reproduced with permission from Izaki and Omi [15]. Copyright (1996) American Institute of Physics)

filmlike structures, perhaps due to the increased growth rate. Interestingly, in a different study where the deposition was galvanostatic (constant current rather than constant potential), a lower current during growth led to well-formed 2D films, while an increased current produced very well-defined 3D nanowires structures (Fig. 5) [31].

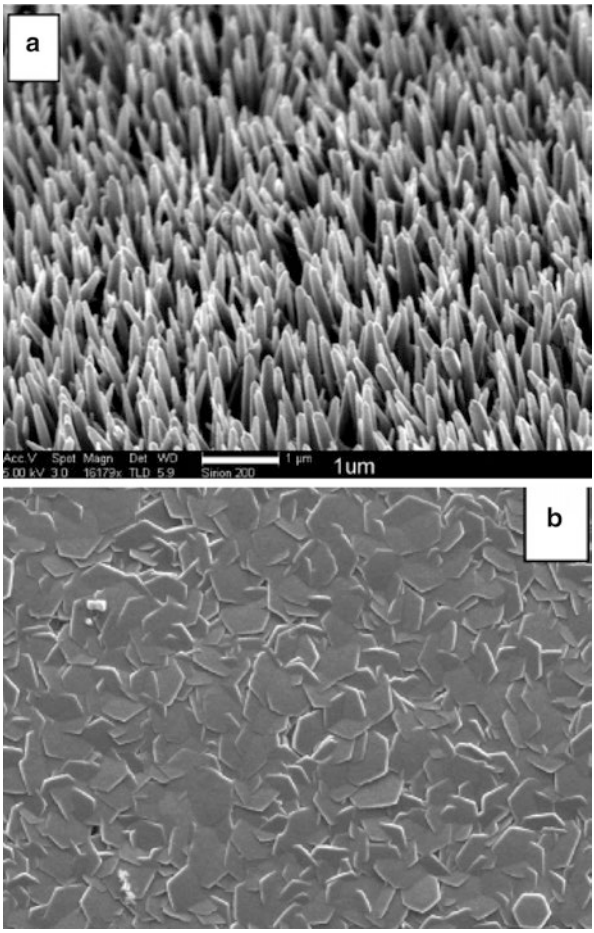

Fig. 5 SEM images of ZnO materials obtained by the zinc nitrate galvanostatic method: (**a**) higher deposition current, (**d**) lower deposition current (Adapted with permission from Cao et al. [31]. Copyright (2006) American Chemical Society)

These ideas were confirmed later in another work on galvanostatic deposition using zinc nitrate when the most uniform and 2D film structures were obtained at quite low deposition currents [32].

Zn^{2+} as a Catalyst for Nitrate Reduction

It would appear as though the zinc nitrate method showcases some inconsistencies and difficulties in obtaining repeatable structures based on certain growth conditions. Recent investigations of the electrochemical growth mechanism in the zinc nitrate method aid in understanding these difficulties.

As discussed already, perhaps the most important aspect of the growth mechanism for ZnO in ECD processes is the local $[Zn^{2+}]/[OH^-]$ ratio at the electrode. Whereas the dissolved oxygen method allows for a broader control of this ratio, in the zinc nitrate method, $[Zn^{2+}]$ and $[OH^-]$ are more difficult to separate. If zinc nitrate is the only source material in the electrolyte, $[Zn^{2+}]$ and $[NO_3^-]$ are

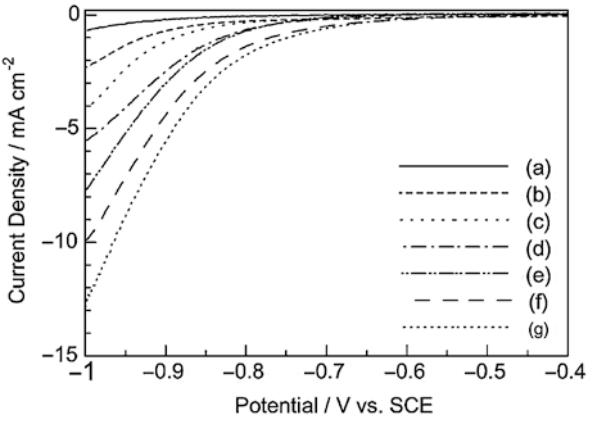

Fig. 6 *I–V* curves measured at a ZnO-coated Pt disk-rotating electrode (500 rev/min) in aqueous mixed solutions of zinc nitrate and potassium nitrate for which the concentration of NO_3^- was fixed at 200 mM while that of Zn^{2+} was varied as (*a*) 0, (*b*) 0.5, (*c*) 2, (*d*) 4, (*e*) 10, (*f*) 20, and (*g*) 100 mM. Potential sweep rate = 5 mV/s (Reproduced with permission from Yoshida et al. [16]. Copyright (2004) Elsevier B.V)

essentially predetermined: it is not immediately possible to independently control $[Zn^{2+}]$, a very important ECD growth parameter. It was discussed in section "ECD ZnO: Dissolved Oxygen Method" that certain ion species affect the electrochemical reduction reaction that governs ZnO deposition in ECD growth processes. The same is true in the zinc nitrate method. It has been very well established that metallic ion species in solution catalyze the nitrate reduction reaction [33, 34]. In fact, without Zn^{2+} present in the zinc nitrate method, the reduction of nitrate electrochemical reaction will not even occur (Fig. 6) [16]. So it becomes clear that while both Zn^{2+} and OH^- are needed to deposit ZnO by ECD, in the zinc nitrate method, these separate ion species are very much interconnected by the catalyst nature of Zn^{2+}. Understandably, this complicates the zinc nitrate method to a certain degree in comparison to the dissolved oxygen process.

Separate NO^{3-} Source in the Zinc Nitrate Method

One strategy developed to overcome this limitation is to utilize a separate source for NO^{3-} ions in the zinc nitrate method [35]. By using sodium nitrate as the main electrolyte precursor, the nitrate concentration can be held constant while the zinc nitrate concentration is changed. What was found in this study was that the zinc nitrate process can become very much like the dissolved oxygen method: low $[Zn^{2+}]$ leads to strongly diffusion-limited growth of ZnO, and high aspect ratio 3D nanowires are obtained. Here, the limited diffusion of Zn^{2+} ions not only minimizes the availability of Zn^{2+} for the reaction with OH^- to produce ZnO but also the catalytic effect for the nitrate reduction reaction to *produce* OH^- ions in the first place. The end result is a very strongly limited growth regime in which the lateral growth of the ZnO structures is completely suppressed, and highly uniform in diameter ZnO

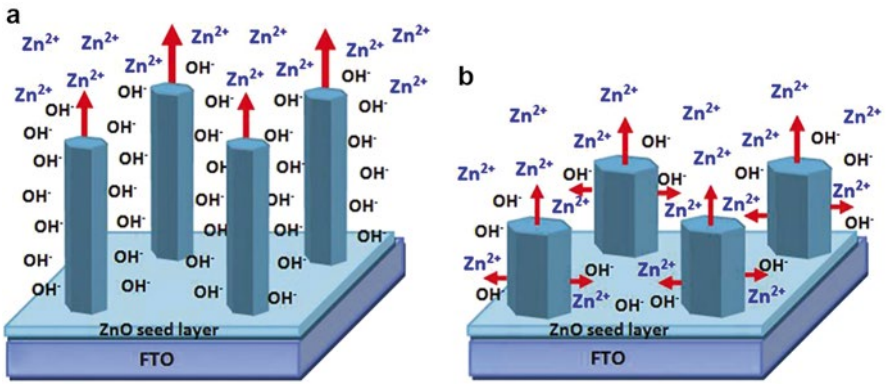

Fig. 7 Schematic view of the growth of ZnO nanowires from nitrate-based solutions. (**a**) The Zn^{2+} diffusion is significantly slower than the OH^- generation rate, and (**b**) the OH^- generation rate and Zn^{2+} diffusion are in the same order (Reproduced with permission from Khajavi et al. [35]. Copyright (2012) Elsevier B.V)

nanowires are obtained (Fig. 7) [35]. By tuning [Zn^{2+}] while keeping other growth conditions constant, it is possible to increase their lateral growth and in turn control the aspect ratio of the ECD ZnO nanowires [35].

Mixed Water/Methanol Electrolytes for Zinc Nitrate ECD

Another strategy related to controlling the availability of Zn^{2+} and OH^- in the zinc nitrate method involves the use of a mixed water/alcohol electrolyte. In this technique, zinc nitrate remains the only source material but instead of a water-only electrolyte, various vol.% of an appropriate cosolvent are added (such as ethanol or methanol) [36, 37]. This technique has been shown to effectively produce very consistent and uniform 2D film structures using the zinc nitrate method across a wide range of other growth conditions [36].

Structural Properties

As is typically found in the literature, when utilizing a water-only deposition solution in the zinc nitrate method, it is difficult to prepare samples with a consistent morphology and homogeneity. Often, scattered and spotty 3D nanorod-type structures that do not eventually form a continuous and hole-/defect-free film are formed [15, 38–41]. An example of the morphologies obtained using a water-only solution is shown in the scanning electron microscopy (SEM) image in Fig. 8a. On the other hand, by simply adding 50 % by volume methanol to the deposition solution, the ZnO morphology is remarkably changed such that a 2D coalesced film made up of compact, hexagonal grains is formed (Figs. 8b, c). Figure 8c is a lower magnification image to showcase the uniformity of and lack of defects in the ZnO film obtained with 50 % methanol.

Furthermore, some of the specific properties of the ZnO films can be controlled with various growth parameters such as applied potential, current density, and

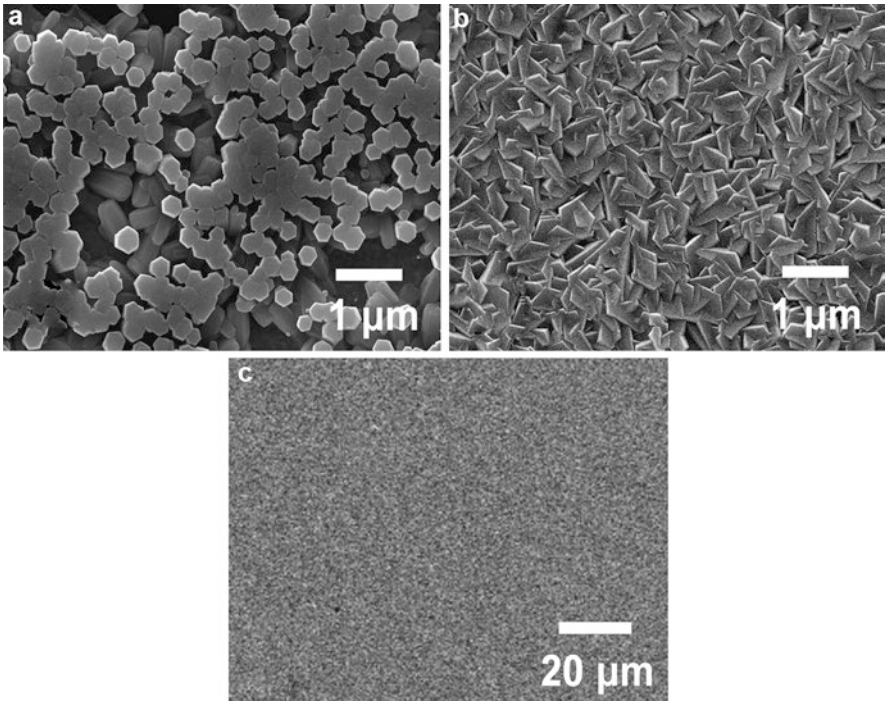

Fig. 8 SEM images of ZnO samples deposited in 0.05 M zinc nitrate solutions: (**a**) 100 % water; (**b**, **c**) 50 % water/50 % methanol (Reproduced with permission from Thomas and Cui [36]. Copyright (2013) The Electrochemical Society)

methanol concentration. Figure 9 shows some of the ZnO films obtained under different growth conditions to modify the specific crystal and film morphology. An increased current density during growth leads to a larger ZnO growth rate and therefore larger crystal grains (Fig. 9a), while a more controlled current density produces smaller and more complete grains (Fig. 9b). The cross section in Fig. 9c shows that the films are very uniform and dense.

Growth Mechanism: CV Analysis and Effects of Methanol

In the combined water/methanol zinc nitrate ECD method, the availability of Zn^{2+} for the deposition of ZnO is quite constant because it comes directly from zinc nitrate and is present at a relatively high concentration (0.05 M). On the other hand, the availability of OH^- is not immediate but instead relies on the reduction of nitrate ions and therefore is dependent on the electrochemical growth conditions.

Figure 10 illustrates CV scans of growth solutions with varying amounts of methanol. Methanol addition does not cause a drastic change in the CV scans; however, the most distinct change visible is the increased current density in the range of potentials used for the deposition of ZnO (highlighted area: −2.4 to −2.6 V). For example, at a potential of −2.5 V, the current density is increased by ~50 %

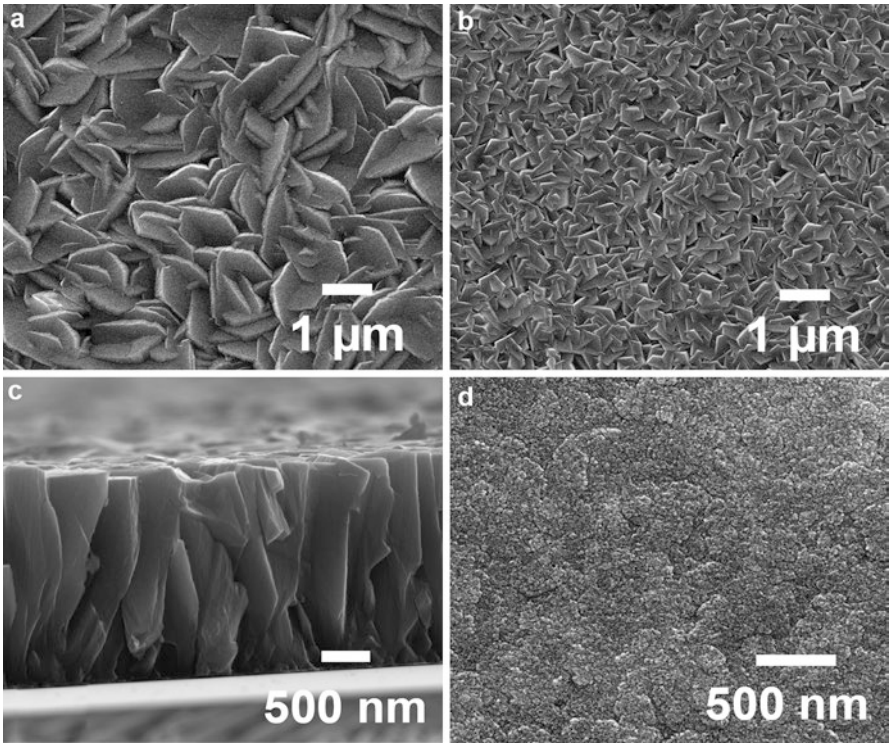

Fig. 9 SEM images of ZnO thin films obtained in a water/methanol zinc nitrate solution: (**a**) −2.5 V, large current density, 50 % methanol; (**b**) −2.5 V, small current density, 50 % methanol; (**c**) cross section of (**a**) 2.2 μm thick film; (**d**) −2.5 V, 25 % methanol (Reproduced with permission from Thomas and Cui [36]. Copyright (2013) The Electrochemical Society)

for the electrolytes with methanol added as compared to the water-only solution. Because the current density should be mostly associated with the nitrate reduction reaction, the CV scans indicate that adding methanol to the ZnO growth solution enhances the nitrate reduction reaction, increasing the production of OH^- ions [36]. Growth solutions with methanol also create a much faster nucleation process, as well as a faster time to coalescence and uniform film growth in general [36]. This likely plays a role in establishing more 2D and uniform film growth dynamics rather than "spotty" growth of 3D nanostructures.

OH^- Ion Production and Thermodynamic Equilibrium

A secondary, yet related, explanation for the improvement in the ZnO film morphology upon methanol addition is an increase in the availability of OH^- ions. When the supply of OH^- ions is slow and steady, a near equilibrium crystallization process for ZnO likely dominates. Recent work on the crystallization of ZnO in solution processes showed that the most important factor for obtaining ZnO nanowire-/nanorod-type structures, i.e., a strongly dominant [0001] crystallization scheme, is the slow and

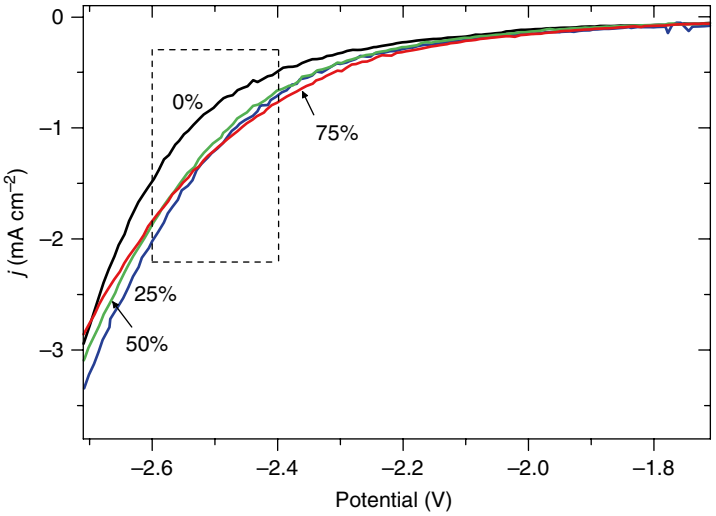

Fig. 10 CV scans of different electrolytes used for ZnO thin film growth. Only the forward scans (0 to −2.7 V) are shown for clarity. The % methanol in the electrolyte is indicated in the figure. Note that all scans were performed at a rate of 20 mV/s on Au substrates (1 cm^2) after a thin layer of ZnO was deposited (5 min growth time) using the respective solution. Only the first scans are shown as no significant change was observed for repeating scans (Reproduced with permission from Thomas and Cui [36]. Copyright (2013) The Electrochemical Society)

steady "release" or availability of OH^- ions to react with Zn^{2+} and make ZnO [42]. This is similar to the minimized availability of Zn^{2+} in the dissolved oxygen method and separate NO_3^- method due to their use of a low $[Zn^{2+}]$.

As a result, it becomes easier to see why ZnO grows preferentially along the [0001] direction and forms nanorod or columnar structures in water-only deposition solutions. The availability of OH^- ions is minimal, producing a growth process that is very much limited by diffusion and thermodynamic equilibrium. However, if the availability of OH^- ions is increased and conditions are shifted outside the realm of equilibrium and diffusion limits, other crystallization schemes can contribute more strongly and the anisotropic [0001] dominated growth may be overcome. This enables more lateral crystal growth and eventually dense, 2D film structures, as outlined in Fig. 7 in section "Separate NO^{3-} Source in the Zinc Nitrate Method."

Chemical Effects of OH^- and Methanol

The chemical effects specific to methanol should also be considered because various ion species were shown to affect the growth of ZnO in the dissolved oxygen method [29]. OH^- ions may also become preferentially associated with the polar (0001) face of the ZnO crystal once their availability is higher. This would be similar to NO_3^- ions as suggested in other work on ECD of ZnO using zinc nitrate in methanol [41] and citrate ions in the hydrothermal growth of ZnO films [43]. Such adsorption of ion species on the polar ZnO crystal faces could drive the growth of

the *non*polar crystal faces and produce a more 2D film structure. In fact, methanol can be used at even higher concentrations in the zinc nitrate method to produce more elaborate structures such as ZnO nanowalls and ZnO nanosheets [41]. This suggests that methanol indeed plays a strong role in the various crystallization schemes for ZnO when used in the zinc nitrate ECD method.

Optical and Electrical Properties: Growth Conditions and Annealing

Optical Properties

The rich optical properties of ZnO materials are very important for their use in advanced optoelectronics. The wide bandgap and large exciton binding energy nature of ZnO leads to strong ultraviolet (UV) luminescence at room temperature as well as the possibility for a range of optical emissions in the visible range.

Optical Quality and Luminescence

In one of the few studies on the effects of growth potential in the dissolved oxygen ECD ZnO method [44], it was established that a lower growth potential, i.e., one that is very close to the limit for O_2 reduction to occur, produces ZnO materials of a higher optical quality. Furthermore, a higher deposition temperature and growth conditions that produce more 3D nanowire-type structures as compared to 2D films also lead to ZnO with an intense UV photoluminescence (PL) emission and very little defect PL emissions. Finally, the use of a Cl^- electrolyte support also benefits the optical properties of ZnO deposited by the dissolved oxygen method [44]. In the zinc nitrate plus hexamine ECD method, it was also shown that the ZnO crystal quality, and in turn optical quality, of ZnO nanowires could be modified by growth conditions such as the applied potential and relative hexamine concentration during growth [45]. More negative growth potentials and a larger relative hexamine concentration lead to ZnO nanowires with a stronger UV emission and very little defects. Much like in the dissolved oxygen method, the addition of Cl^- to the electrolyte in the zinc nitrate plus hexamine process enables filling of native defects with Cl impurities and the removal of defect PL emissions [46].

Bandgap Tuning

Another key parameter with regard to ZnO's optical properties is its bandgap energy. Because ZnO maintains such a wide bandgap, the ability to modulate the bandgap even further into the UV as well as into the visible region becomes highly desirable. Interestingly, several studies have shown that the bandgap of ECD ZnO materials is highly tunable with specific growth conditions as well as doping. The results on doped ZnO will be discussed at length further in the chapter, but even undoped ECD ZnO can show a range of bandgaps by changing the applied potential during growth [47]. The ZnO bandgap is tunable within a range of about 0.2 eV with wider bandgaps being associated with more negative growth potentials.

Electrical Properties and Electrical Characterization Techniques

A sound understanding of the electrical properties of ECD ZnO materials is paramount to their eventual application in advanced devices. Unfortunately, ECD processes demand the use of a conductive substrate, stifling the ability to perform standard semiconductor electrical characterization without complications and errors.

Thin Film Transfer

Efforts have been made in the past to isolate semiconductor thin films obtained by ECD methods from their conductive substrate, most notably on solar cell materials such as CdTe [48], CdS [48], CIS [49], and Cu_2O [50]. Upon successful film transfer, resistivity and Hall effect measurements can be carried out as with any other semiconductor material. Only very recently have such methods been demonstrated with regard to ECD ZnO, and finally there are viable data available for the electrical properties of ZnO materials obtained by electrochemical methods [36, 51, 52].

Electrochemistry-Based Characterization Techniques

Another approach is associated with electrochemical impedance spectroscopy (EIS) and Mott–Schottky analysis (MS) in which the conductive growth substrate required for ECD processes is actually utilized in the electrical measurement. A wide variety of ZnO thin films and even 3D nanowire structures have been characterized by such EIS and MS methods [26, 27, 36, 38, 41, 53, 54]. For more details regarding the theory and practice of EIS and MS analysis, see Refs. [27, 36, 38, 53].

The final technique for characterizing the electrical properties of ECD materials is a photoelectrochemical cell (PEC) measurement [55–57]. This method cannot provide any detailed quantitative information regarding charge carrier concentration or mobility, but it can give qualitative insight into the conductivity type and relative magnitude of carriers. A PEC measurement involves a semiconductor and an electrolyte interface, and the charge transfer between the two is monitored upon illumination of the semiconductor with an external light source. A schematic of a typical PEC setup is shown in Fig. 11. A positive change in potential signifies *p*-type behavior, while a negative voltage change indicates *n*-type properties. Both ZnO thin films [58, 59] and nanowires [57] have been characterized by PEC measurements in order to gain information regarding their conductivity type and capability.

Specific Results on Various ECD ZnO Materials

While the available work on the electrical properties of ECD ZnO is somewhat minimal, certain trends and consistencies are beginning to develop. Highly uniform and dense 2D films grown by the dissolved oxygen method have shown electron concentrations close to the 10^{20} cm^{-3} range when highly doped with Cl [27]. Meanwhile, the same study found that films deposited by the zinc nitrate method were also *n*-type, but had electron concentrations nearly two orders of magnitude lower than those obtained in the standard dissolved oxygen process [27].

The electrical properties of ZnO nanowires obtained by the dissolved oxygen method have also been explored with EIS and MS. It is necessary to modify the

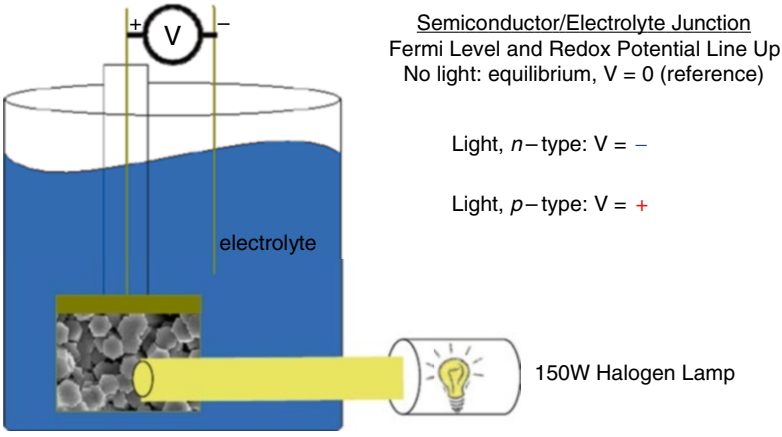

Fig. 11 Schematic of the PEC measurement setup and basic principles

analysis in order to compensate for the 3D geometry of the nanowires [53], but very consistent data has been obtained by a variety of groups [26, 53, 54]. As-grown ZnO nanowires by the dissolved oxygen method are typically highly *n*-type, with carrier concentrations at least in the 10^{19} cm^{-3} range [26, 53, 54]. This may stem from the fact that Cl doping takes place due to the Cl^- supporting electrolyte. Similar experiments have been performed on ZnO nanowires obtained by the zinc nitrate plus hexamine method, and they show that undoped nanowires have carrier concentrations in the mid-10^{17} cm^{-3} range [60]. Then, purposeful Cl doping can be utilized to increase their electron concentration to the mid-10^{20} cm^{-3} range [60]. It seems Cl doping is very much a part of the electrical properties of ECD ZnO nanowires, whether it is desired or not. In related studies [26], it was shown that Cl^- ions in particular inhibit the O_2 reduction reaction, which lowers the production of OH^- ions and alters the $[Zn^{2+}]/[OH^-]$ ratio during growth. The increased availability of Zn^{2+} in comparison to OH^- leads to more "Zn heavy" ZnO nanowires with an increased electron concentration due to zinc interstitial and oxygen vacancy defects [26].

The electrical properties of ZnO materials obtained by the zinc nitrate method have also been investigated. In this case, both MS and Hall effect measurements have been used so a more complete picture of the electrical properties can be seen. The applied potential during growth has been shown to be a very strong factor in determining the electrical properties of ECD ZnO obtained by nitrate reduction. Figure 12 displays the calculated carrier concentration values obtained from MS analysis for several ZnO films as a function of the applied potential used during growth (zinc nitrate in 50 % methanol). Three different films all deposited at −2.4 V are included in the data to show that the samples have reasonably consistent carrier concentrations for a given applied potential (−2.4 V ranges from 9.6×10^{15} to 2.9×10^{16} cm^{-3}). A lower applied potential, which also corresponds to a lower current density and growth rate, produces ZnO films with higher carrier concentrations. Meanwhile, a more negative growth potential leads to a faster ZnO growth rate as well as lower carrier concentrations.

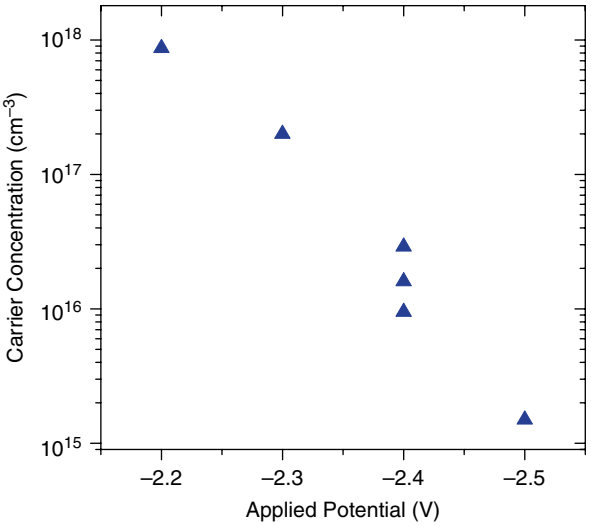

Fig. 12 Carrier concentration data calculated from MS plots of ZnO films deposited by the zinc nitrate plus methanol method as a function of applied potential during growth (Reproduced with permission from Thomas and Cui [36]. Copyright (2013) The Electrochemical Society)

The range of carrier concentrations for growth potentials from −2.2 to −2.5 V extends through nearly three orders of magnitude [36].

Other works on ZnO films obtained by nitrate reduction found highly similar results when the effects of current density on electrical properties were tested: a lower current density during growth produces ZnO films with higher carrier concentrations as measured by the Hall effect [52]. Changes in the current density alone enabled a similar three orders of magnitude control of the electron concentration of the ZnO films (Fig. 13) [52]. Previous work on ZnO by nitrate reduction using MS analysis has also shown that more negative growth potentials produce lower carrier concentrations with a three orders of magnitude range controlled by the potential [38].

A likely explanation for the observed carrier concentration changes is the growth conditions for ZnO associated with an increased current density and/or more negative growth potentials. Such conditions are related to an increased availability of OH^- ions from an enhanced nitrate reduction process. More OH^- ions may shift the ZnO growth conditions toward a more even Zn/O ratio in that there is plenty of the oxygen source (OH^-) available for stoichiometric ZnO crystallization.

Annealing Effects

Because of their very-low-temperature deposition, moderate annealing has been shown to affect the various properties of ECD ZnO materials as well. MS analysis of ZnO films from the zinc nitrate in 50 % methanol method annealed at 200 °C in air reveals that they possess carrier concentrations as much as two orders of

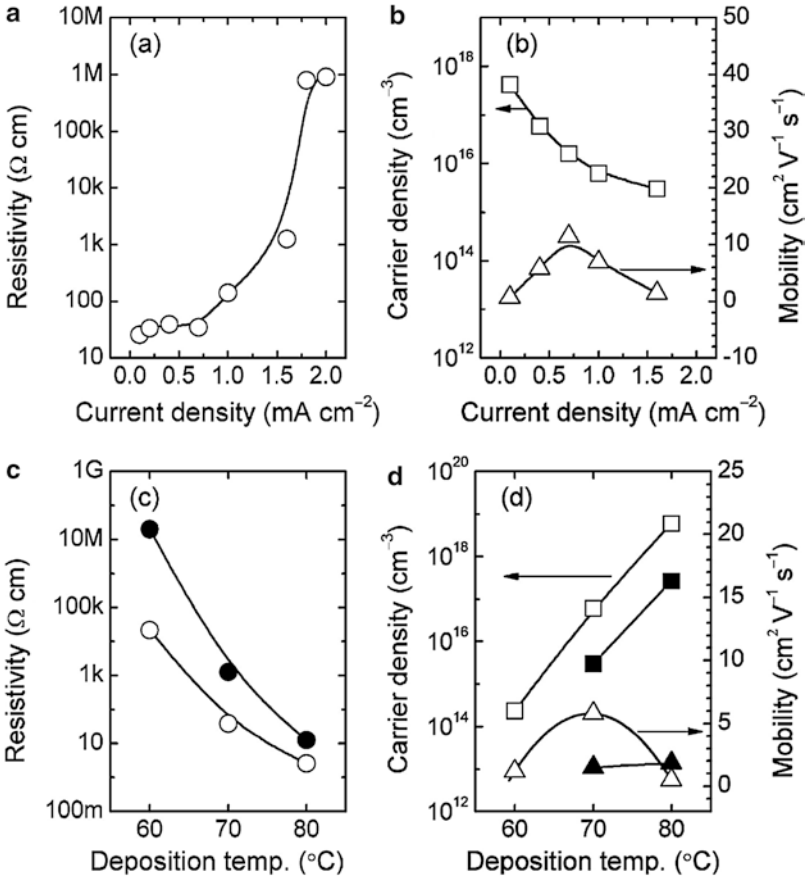

Fig. 13 Variation of electrical properties of electrodeposited ZnO films as a function of (**a**, **b**) current density and (**c**, **d**) deposition temperature (Reproduced with permission from Shinagawa et al. [52]. Copyright (2012) American Chemical Society)

magnitude higher than the as-grown films (annealed in air: high 10^{17} to low 10^{18} cm^{-3}) [36]. The increase in free carriers is partially dependent on the films' as-grown properties – those samples with lower as-grown carrier concentrations experience the most drastic increase in carrier concentration upon annealing.

Hall effect analysis from the same study indicates similar trends: some of the typical resistivities measured for such ZnO thin films are shown in Fig. 14. It is clear that as-grown films are highly resistive, while moderate annealing in air can improve their conductivity. Some other works on ZnO thin films by nitrate reduction have indicated a similar increase in conductivity after moderate annealing [51, 52], but the opposite seems to be true for ZnO nanowires obtained by ECD and then annealed in air [26, 53, 54]. It is interesting that as-grown nanowires by ECD have high electron concentrations and annealing can make them more "intrinsic," in fact lowering their carrier density by as much as three orders of magnitude. Meanwhile, as-grown

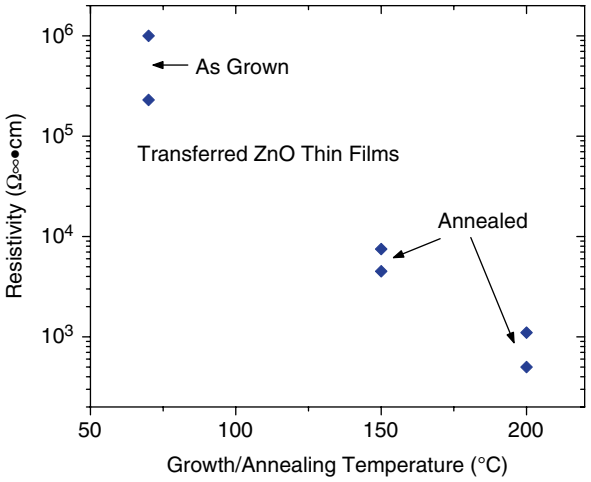

Fig. 14 Measured resistivity values for as-grown and annealed ZnO thin films after the thin film transfer process. All films were deposited at either −2.4 or −2.5 V in 50 % methanol solutions (Reproduced with permission from Thomas and Cui [36]. Copyright (2013) The Electrochemical Society)

films by ECD are often highly resistive, but moderate annealing improves their conductivity. It is clear that the growth conditions leading to either 3D nanowires or 2D film structures also affect the electrical properties of ECD ZnO.

ECD ZnO: Doping for Device Applications

Electrochemical Doping of ZnO

The idea to dope ZnO utilizing low-temperature, electrochemical growth methods is certainly not new. Once the original methods for obtaining nominally undoped ZnO by ECD were established, work on doping ZnO by similar processes soon followed. To date, more than 17 dopants have been tested by various ECD growth processes for ZnO. In most cases, the purpose of the doping is to modulate the optical and/or electrical properties of the ZnO materials. For example, dopants such as Al [61, 62], Ga [61], In [62, 63], B [64], Cl [26, 27, 60, 65], and Y [66] were all expected to enhance the native *n*-type conductivity of ZnO. Dopants like Cd, Mg, and Eu have been shown to modify the optical properties of ZnO by changing its bandgap (Cd, Mg) [67–70] or utilizing excited state transitions of the dopant (Eu) [70]. In addition, a few particular dopants such as Ni [71], Co [71, 72], Fe [73], and Mn [74] were focused on introducing ferromagnetic properties into the ZnO materials for the purpose of creating dilute magnetic semiconductors (DMS).

There has been less work on *p*-type doping of ZnO by electrochemical methods, with only Ag-doped ZnO being tested recently [57, 75, 76]. Other low-temperature solution methods (hydrothermal) have been explored more in this regard, with Sb as the most common dopant [77, 78]. Others such as K [79], P [80], Ag [78], and Li [81] have been investigated as well. Some of the more thorough and enhanced work on electrochemical doping of ZnO is summarized here with focus on *n*-type and *p*-type dopants.

n-Type Doping with Cl

While *n*-type doping of ZnO using ECD methods has been explored significantly, the most successful and consistent results are associated with Cl doping. In particular, the dissolved oxygen ECD method has been used to dope both ZnO thin films [27] and nanowires [26] with Cl, in part because Cl^- or ClO_4^- ions are naturally present in the supporting electrolyte. In fact, when a chlorine-containing electrolyte is used in the dissolved oxygen method, it is essentially impossible to avoid Cl doping in the ECD growth process. Naturally, such ECD ZnO materials become highly *n*-type with enhanced electron concentrations [26]. Upon further addition of Cl to the growth process, carrier concentrations as high as 9×10^{19} cm^{-3} for 2D films [27] and 4×10^{20} cm^{-3} for 3D nanowires [26] can be achieved. Such materials are excellent candidates for transparent conductor applications in solar cells and LEDs. In fact, Cl-doped ZnO films by ECD have been utilized as a top contact layer in solar cells [65]. Cl doping also widens the bandgap of both ZnO thin films [27] and nanowires [46, 60].

p-Type Doping with Ag

Among various potential dopant materials, Ag has demonstrated its suitability for *p*-type doping of ZnO. So far, Ag-doped ZnO nanostructures and thin films have been explored by many techniques, but very few were low-temperature and/or solution-based methods [78, 82]. In many cases of the high-temperature methods, the Ag-doped materials showed *p*-type conductivity [83–85]; however, there is certainly not a guarantee that successful Ag doping of ZnO will lead to *p*-type behavior [86]. Achieving *p*-type ZnO via solution-based methods at lower deposition temperatures has proven to be more difficult.

In the past several years strides have been made in *p*-type doping of ZnO by ECD processes with Ag doping in the zinc nitrate plus hexamine process [57, 75, 76]. As was mentioned above, the zinc nitrate plus hexamine process tends to produce ZnO nanowires, and in the undoped case their background electron concentrations are not too high (~10^{17} cm^{-3}) [60]. Therefore, the zinc nitrate plus hexamine method provides an excellent starting point for *p*-type doping.

Effects of Ag^+ on ECD Growth Process

Ag^+ maintains a much stronger influence on the ECD growth process than many other additive ions have shown in previous work. Whereas Cl^-, ClO_4^-, SO_4^{2-}, and acetate ions can all be added to the ECD growth solution to relatively high concentrations (0.1 M) [26–28], the addition of Ag^+ must be much more closely monitored and controlled. Basically, even at concentrations of only 1–5 % relative to Zn^{2+}, Ag^+ disrupts the normal ZnO nanowire growth process, making the deposition of highly uniform Ag-doped ZnO materials difficult [87]. Investigations with CV analysis show that Ag^+ catalyzes the nitrate reduction electrochemical reaction much like Zn^{2+}, perhaps even more so [76].

Figure 15 shows CV scans of various zinc nitrate plus hexamine electrolytes with different amounts of Ag^+ added. It is clear that even at a very low relative concentration of 0.05 %, Ag^+ strongly affects the nitrate reduction reaction, enhancing the cathodic current significantly [76]. Figure 16 displays the measured deposition

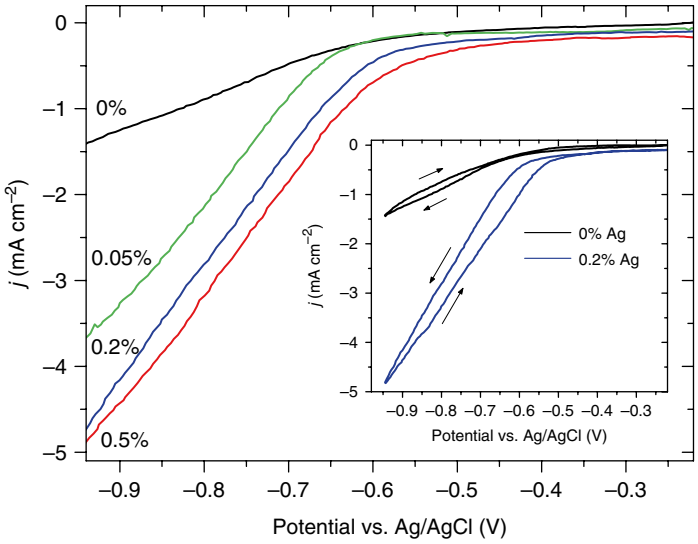

Fig. 15 CV scans of the electrolytes used for undoped and Ag-doped ZnO nanowire growth. The mol.% of Ag in the growth solution is indicated in the figure. Only the forward scans (0 → −0.95 V) are shown for clarity. The inset shows full CV scans for the 0 and 0.2 % Ag solutions (Reproduced with permission from Thomas et al. [76]. Copyright (2012) American Chemical Society)

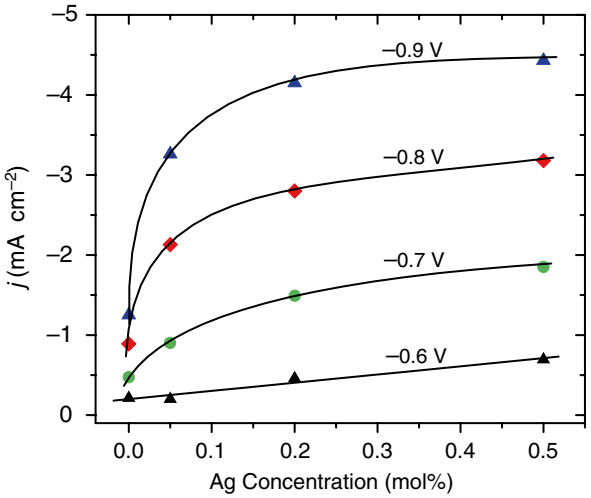

Fig. 16 Current density versus Ag concentration in the ZnO nanowire growth solution at different applied potentials. The data are taken from the CV scans in Fig. 17. The solid lines are simply guides for the eye (Reproduced with permission from [76]. Copyright (2012) American Chemical Society)

currents at various applied potentials along with the effects of Ag^+ at different concentrations. At larger negative potentials, the influence of Ag^+ is even more pronounced at the lowest concentration, indicating its true nature as a catalyst for nitrate reduction [76].

Structure and Morphology

The overall result of the catalyst nature of Ag^+ is simply that growth conditions such as [Ag^+] and the applied potential must be well optimized for efficient doping of Ag into ZnO nanowires. The well-controlled and uniform growth of ZnO nanowires needs to be maintained, yet sufficient Ag doping must also occur in order to obtain *p*-type properties. Such conditions include a low Ag concentration in the growth solution (0.05–0.5 %) as well as a minimized current density.

Figure 17 shows representative SEM images of the undoped and Ag-doped nanowire arrays obtained by ECD under more controlled growth conditions. The nanowires have diameters of 100–200 nm and lengths ranging from 0.7 to 2.5 μm depending on the specific growth parameters. Under these milder growth conditions, the ZnO nanowire morphologies are not significantly affected by Ag doping. However, as discussed above, it is possible to drastically modify the morphologies of the Ag-doped ZnO nanomaterials by using higher Ag concentrations and potentials [87].

Ag Doping Levels: ECD Growth Conditions

An approximately linear increase in the Ag content of the nanowires is observed as the Ag concentration is increased in the electrolyte (Fig. 18). The actual Ag content in the doped nanowires is much larger than the Ag concentration in the growth solution, indicating Ag is readily incorporated into the ZnO nanowires even at a very low concentration relative to Zn in the electrolyte. The enhanced catalytic role of Ag^+ in the electrochemical growth process may help to explain this observation: much like Zn^{2+}, Ag^+ is adsorbed onto the electrode (ZnO nanowire) surface where it acts as a catalyst for the reduction of nitrate [76]. The CV analysis suggests Ag^+ is a more efficient catalyst than Zn^{2+} for nitrate reduction; therefore, it may be more easily incorporated into ZnO than Zn despite its very low concentration relative to Zn.

Because of the very low concentration of Ag relative to Zn, Ag incorporation is also highly limited by diffusion. As a result, the nanowire growth rate affects the final Ag content because faster ZnO deposition limits the possibility for Ag incorporation. This likely explains the trend of lower Ag contents in the samples deposited at more negative potentials but the same Ag concentration (Fig. 18). ZnO doped with other materials by ECD methods has shown similar behavior [62–64], suggesting the electrochemical doping process in ZnO maintains universal traits.

Optical and Electrical Properties: Evidence for *p*-Type Doping

The PL properties of ECD Ag-doped ZnO have also been investigated [57, 75]. Samples grown at increased applied potentials were very different from undoped ZnO with respect to their defect emission in the visible and near-band edge (NBE) emission in the near-UV range. These changes indicate that Ag doping enhances

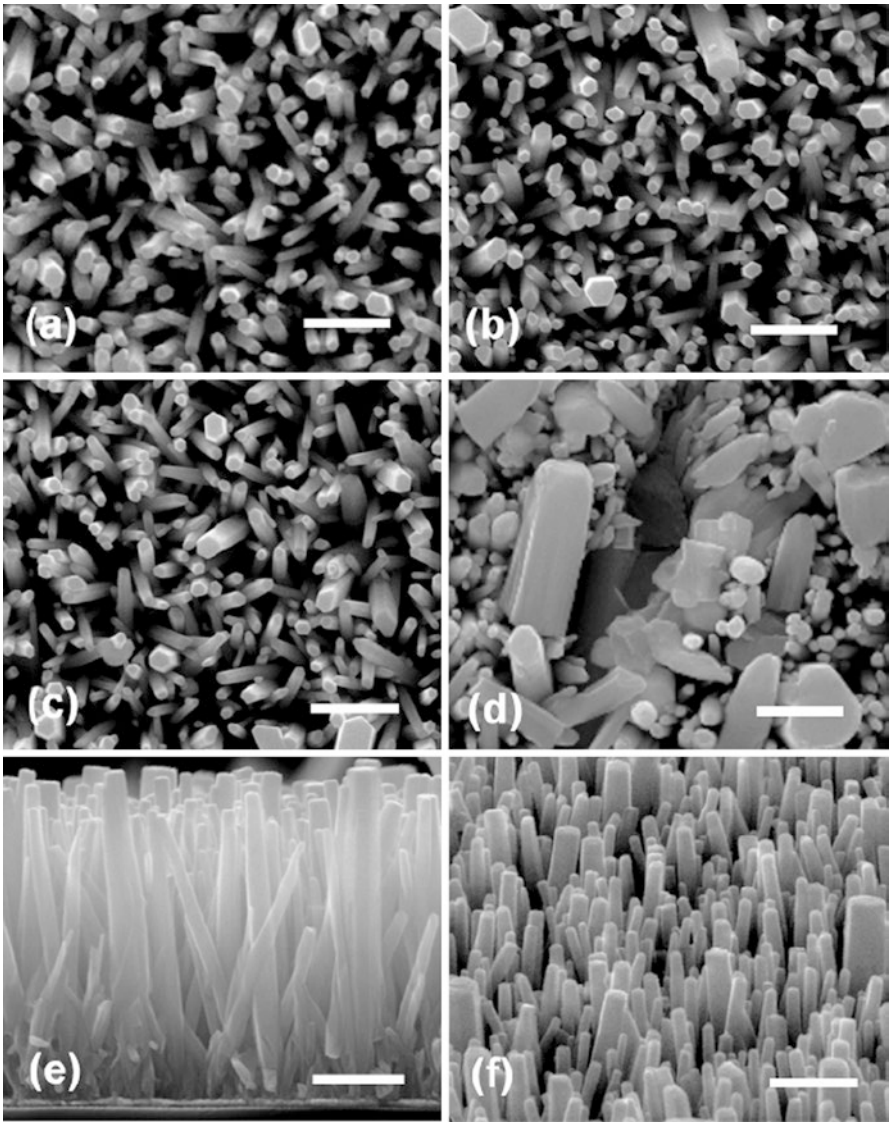

Fig. 17 SEM images of (**a**) undoped and (**b**–**f**) Ag-doped ZnO nanowires. The growth conditions are as follows: (**a**) -0.7 V, 0 % Ag; (**b**) -0.7 V, 0.05 % Ag; (**c**) -0.7 V, 0.2 % Ag; (**d**) -0.8 V, 1 % Ag. (**e**, **f**) are a cross section and tilted view of the sample in (**c**). The scale bar in each figure is 500 nm. Note that all deposition potentials are reported relative to an Ag/AgCl reference electrode (Adapted with permission from Thomas and Cui [57]. Copyright (2010) American Chemical Society)

the concentration of native defects during the nanowire growth process and also may establish a reduced bandgap in ZnO [57, 75]. Intense emissions at low temperature of a free electron to neutral acceptor transition at 3.323 eV were present in Ag-doped samples grown at more negative potentials, while a donor-bound

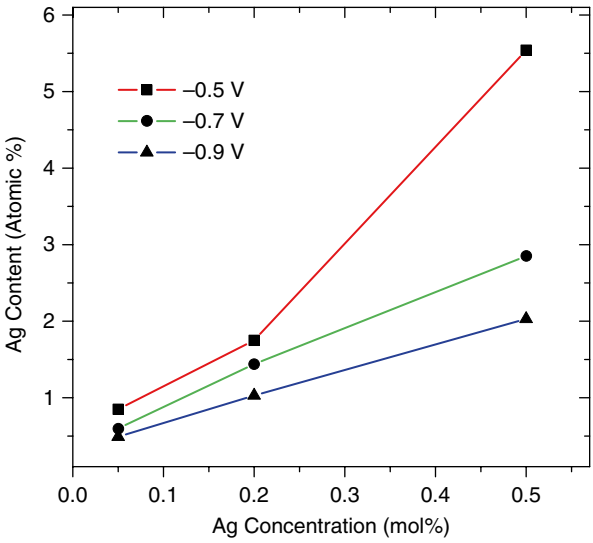

Fig. 18 Ag content measured by energy dispersive x-ray spectroscopy in the doped ZnO nanowires as a function of Ag concentration in the growth solution (Reproduced with permission from Thomas et al. [76]. Copyright (2012) American Chemical Society)

exciton emission dominated the band edge emission for undoped ZnO [75]. Temperature-dependent PL measurements allowed for the calculation of a binding energy of 117 meV for the acceptor involved in the transition at 3.323 eV [75]. The incorporation of Ag into ZnO enhanced the acceptor-related emission, although it is not clear whether this enhancement directly results from Ag impurities or native defects. The optical properties' results provide evidence that Ag is a potential *p*-type dopant for ZnO.

The electrical properties of the undoped and Ag-doped ZnO nanowires were also explored with a solution-based PEC technique. Both as-grown-doped and undoped nanowires have negative PEC responses upon illumination (*n*-type conductivity, Fig. 19). However, the doped samples tend to show a smaller magnitude of the negative PEC signal, indicating a possible decrease in donors and increase in acceptors in these samples due to Ag doping. The annealed Ag-doped nanowires display significant changes in their PEC responses depending on their growth conditions. Much like the PL results, Ag-doped samples grown at more negative applied potentials were distinct from undoped and other Ag-doped nanowires. These samples showed positive PEC responses, a strong indicator of *p*-type electrical properties [57]. Ag-doped samples grown at more negative growth potentials and annealed at moderate temperatures in air (350 °C) showed the most enhanced *p*-type properties [76]. The *p*-type properties of the nanowires were very repeatable under appropriate growth conditions and were also stable over long periods of sample storage. The key factors in producing Ag-doped ZnO with strong evidence of *p*-type properties from both optical and electrical characterization included sufficient Ag doping, improved crystalline quality from moderate annealing, and minimized effects of Ag^+ on the ECD growth process [57, 76].

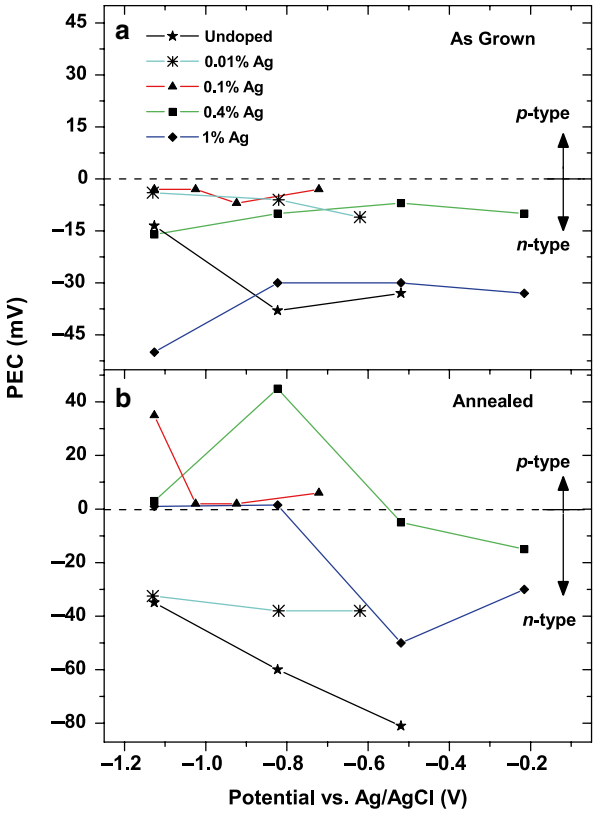

Fig. 19 PEC responses for (**a**) as-grown and (**b**) annealed (600 °C) samples. The mol.% of Ag in the growth solution is indicated in the figure (Reproduced with permission from Thomas and Cui [57]. Copyright (2010) American Chemical Society)

p-Type Doping Mechanism

It is possible that electrochemical growth parameters such as the applied potential and presence of Ag^+ can modulate the deposition conditions for ZnO, favoring either Zn-rich or O-rich environments. Certainly, as the deposition proceeds and ZnO is formed, some of the Zn is used up, in principle lowering the $[Zn^{2+}]/[OH^-]$ ratio. This should be true especially for larger growth rates. At larger negative potentials and with Ag^+ present, the ZnO growth rate is the highest, leading to the fastest use of the available Zn. The availability of OH^- from the electrochemical reduction of nitrate ions is also highly dependent on the applied potential, and from the CV analysis for Ag-doped growth solutions (Fig. 17), it is clear that the presence of Ag^+ creates a similar increase in the rate of nitrate reduction. Therefore, as the applied potential is increased negatively and Ag^+ is added to the electrolyte, the production of OH^- ions is substantially increased, and the $[Zn^{2+}]/[OH^-]$ ratio may decrease considerably. These combined effects shift the growth conditions toward an O-rich environment, in turn altering the native defect and Ag impurity formation mechanisms in the nanowires [76]. O-rich conditions are expected to minimize the formation of native donor defects (Zn_i, V_O) [88, 89] while also lowering the formation energy for native acceptor defects (V_{Zn}, O^i) [88, 89] and Ag impurities [90–92].

These ideas could help to explain the results discussed above where Ag-doped nanowires with *p*-type properties were mainly obtained at a potential more negative than –0.65 V [57], and the optimal *p*-type properties were associated with a larger negative potential (–0.9 V) and moderate annealing temperature of 350 °C [76]. Similarly, even in undoped ZnO nanowires, their PEC responses indicated reduced *n*-type character at more negative growth potentials, which fits well with the discussion here and in section "Electrical Properties and Electrical Characterization Techniques."

Summary and Outlook

From their humble beginnings almost 20 years ago, ECD processes for ZnO have become an increasingly important choice among the various techniques for fabricating ZnO materials. The low cost and low-temperature nature of ECD, along with its amenability to large-scale production, suggests it will only continue to gain interest in the future. The electrochemical growth mechanisms associated with ECD ZnO processes are now very well understood. Regardless of the specific ECD method used, the local ZnO growth environment, specifically the $[Zn^{2+}]/[OH^{-}]$ ratio, has been demonstrated to be the single most important parameter for governing the properties of ECD ZnO materials. Many strategies can be used to alter these conditions, such as changing the growth potential, adjusting initial precursor concentrations, and including additives with the standard ECD electrolyte. As a result of these modifications, it has become possible to control the structural, optical, and electrical properties of ZnO for use in a range of advanced device applications. ECD ZnO materials have been integrated into solar cells [65, 93–95], LEDs [68, 96], photonics [97], and DMS applications [71, 72], just to name a few.

The future of ECD ZnO is bright, with new opportunities to further improve the quality and variety of ZnO structures, sharpen controlled fabrication methods for tunable 1D and 2D arrays, and modulate the electrical properties of thin films and nanomaterials for use in low-cost optoelectronics.

References

1. Reynolds DC, Look DC, Jogai B, Jones RL, Litton CW, Harsch W, Cantwell G (1999) Optical properties of ZnO crystals containing internal strains. J Lumin 82:173
2. Ozgur U, Alivov YI, Liu C, Teke A, Reshchikov MA, Dogan S, Avrutin V, Cho SJ, Morkoc H (2005) A comprehensive review of ZnO materials and devices. J Appl Phys 98:103
3. Look DC, Reynolds DC, Litton CW, Jones RL, Eason DB, Cantwell G (2002) Characterization of homepitaxial p-type ZnO grown by molecular beam epitaxy. Appl Phys Lett 81:1830
4. Wu JJ, Liu SC (2002) Low-temperature growth of well-aligned ZnO nanorods by chemical vapor deposition. Adv Mater 14:215
5. Sun XW, Kwok HS (1999) Optical properties of epitaxially grown zinc oxide films on sapphire by pulsed laser deposition. J Appl Phys 86:408
6. Kaidashev EM, Lorenz M, von Wenckstern H, Rahm A, Semmelhack HC, Han KH, Benndorf G, Bundesmann C, Hochmuth H, Grundmann M (2003) High electron mobility of epitaxial

ZnO thin films on c-plane sapphire grown by multistep pulsed-laser deposition. Appl Phys Lett 82:3901
7. Pan ZW, Dai ZR, Wang ZL (2001) Nanobelts of semiconducting oxides. Science 291:1947
8. Lin BX, Fu ZX, Jia YB (2001) Green luminescent center in undoped zinc oxide films deposited on silicon substrates. Appl Phys Lett 79:943
9. Ohshima E, Ogino H, Niikura I, Maeda K, Sato M, Ito M, Fukuda T (2004) J Cryst Growth 260:166
10. Triboulet R, Munoz-Sanjose V, Tena-Zaera R, Martinez-Thomas MC, Hassani S (2005) In: Nickel NH, Terukov E (eds) Zinc oxide – a material for micro- and optoelectronic applications. NATO science series II, vol 194. Springer, Berlin, pp 3–14
11. Reynolds DC, Litton CW, Look DC, Hoelscher JE, Claflin B, Collins TC, Nause J, Nemeth B (2004) High-quality, melt-grown ZnO single crystals. J Appl Phys 95:4802
12. Lincot D (2010) Solution growth of functional zinc oxide films and nanostructures. MRS Bull 35:778
13. Schmidt-Mende L, MacManus-Driscoll JL (2007) ZnO – nanostructures, defects, and devices. Mater Today 10:40
14. Peulon S, Lincot D (1996) Cathodic electrodeposition from aqueous solution of dense or open-structured zinc oxide films. Adv Mater 8:166
15. Izaki M, Omi T (1996) Transparent zinc oxide films prepared by electrochemical reaction. Appl Phys Lett 68:2439
16. Yoshida T, Komatsu D, Shimokawa N, Minoura H (2004) Mechanism of cathodic electrodeposition of zinc oxide thin films from aqueous zinc nitrate baths. Thin Solid Films 451:166
17. Ashfold MNR, Doherty RP, Ndifor-Angwafor NG, Riley DJ, Sun Y (2007) The kinetics of the hydrothermal growth of ZnO nanostructures. Thin Solid Films 515:8679
18. McPeak KM, Becker MA, Britton NG, Majidi H, Bunker BA, Baxter JB (2010) In situ X-ray absorption near-edge structure spectroscopy of ZnO nanowire growth during chemical bath deposition. Chem Mater 22:6162
19. Pauporte T, Lincot D (2001) Hydrogen peroxide oxygen precursor for zinc oxide electrodeposition I. Deposition in perchlorate medium. J Electrochem Soc 148:C310
20. Pauporte T, Lincot D (2001) Hydrogen peroxide oxygen precursor for zinc oxide electrodeposition II – Mechanistic aspects. J Electroanal Chem 517:54
21. Vayssieres L (2003) Growth of arrayed nanorods and nanowires of ZnO from aqueous solutions. Adv Mater 15:464
22. Vayssieres L, Keis K, Hagfeldt A, Lindquist SE (2001) Three-dimensional array of highly oriented crystalline ZnO microtubes. Chem Mater 13:4395
23. Vayssieres L, Keis K, Lindquist SE, Hagfeldt A (2001) Purpose-built anisotropic metal oxide material: 3D highly oriented microrod array of ZnO. J Phys Chem B 105:3350
24. Greene LE, Law M, Goldberger J, Kim F, Johnson JC, Zhang YF, Saykally RJ, Yang PD (2003) Low-temperature wafer-scale production of ZnO nanowire arrays. Angew Chem Int Ed 42:3031
25. Cui JB, Gibson UJ (2005) Enhanced nucleation, growth rate, and dopant incorporation in ZnO nanowires. J Phys Chem B 109:22074
26. Tena-Zaera R, Elias J, Levy-Clement C, Bekeny C, Voss T, Mora-Sero I, Bisquert J (2008) Influence of the potassium chloride concentration on the physical properties of electrodeposited ZnO nanowire arrays. J Phys Chem C 112:16318
27. Rousset J, Saucedo E, Lincot D (2009) Extrinsic doping of electrodeposited zinc oxide films by chlorine for transparent conductive oxide applications. Chem Mater 21:534
28. Elias J, Tena-Zaera R, Levy-Clement C (2008) Electrochemical deposition of ZnO nanowire arrays with tailored dimensions. J Electroanal Chem 621:171
29. Elias J, Tena-Zaera R, Levy-Clement C (2008) Effect of the chemical nature of the anions on the electrodeposition of ZnO nanowire arrays. J Phys Chem C 112:5736
30. Xu F, Lu YN, Xia LL, Xie Y, Dai M, Liu YF (2009) Seed layer-free electrodeposition of well-aligned ZnO submicron rod arrays via a simple aqueous electrolyte. MRS Bull 44:1700

31. Cao BQ, Li Y, Duan GT, Cai WP (2006) Growth of ZnO nanoneedle arrays with strong ultraviolet emissions by an electrochemical deposition method. Cryst Growth Des 6:1091
32. Ashida A, Fujita A, Shim YG, Wakita K, Nakahira A (2008) ZnO thin films epitaxially grown by electrochemical deposition method with constant current. Thin Solid Films 517:1461
33. Cox JA, Brajter A (1979) Mechanisms of ZR(IV) and LA(III) catalysis of the reduction of nitrate at mercury. Electrochim Acta 24:517
34. Ogawa N, Ikeda S (1991) On the electrochemical reduction of nitrate ion in the presence of various metal ions. Anal Sci 7(Suppl):1681
35. Khajavi MR, Blackwood DJ, Cabanero G, Tena-Zaera R (2012) New insight into growth mechanism of ZnO nanowires electrodeposited from nitrate-based solutions. Electrochim Acta 69:181
36. Thomas MA, Cui JB (2013) Highly Uniform 2D Growth, Substrate Transfer, and Electrical Characterization of Electrodeposited ZnO Thin Films. J Electrochem Soc 160:D218
37. Musselman KP, Gershon T, Schmidt-Mende L, MacManus-Driscoll JL (2011) Macroscopically uniform electrodeposited ZnO films on conducting glass by surface tension modification and consequent demonstration of significantly improved p-n heterojunctions. Electrochim Acta 56:3758
38. Chatman S, Emberley L, Poduska KM (2009) Significant carrier concentration changes in native electrodeposited ZnO. ACS Appl Mater Interfaces 1:2348
39. Izaki M (1999) Preparation of transparent and conductive zinc oxide films by optimization of the two-step electrolysis technique. J Electrochem Soc 146:4517
40. Zhang LS, Chen ZG, Tang YW, Jia ZJ (2005) Low temperature cathodic electrodeposition of nanocrystalline zinc oxide thin films. Thin Solid Films 492:24
41. Wu KY, Sun ZQ, Cui JB (2012) Unique approach toward ZnO growth with tunable properties: influence of methanol in an electrochemical process. Cryst Growth Des 12:2864
42. McPeak KM, Le TP, Britton NG, Nicholov ZS, Elabd YA, Baxter JB (2011) Chemical bath deposition of ZnO nanowires at near-neutral pH conditions without hexamethylenetetramine (HMTA): understanding the role of HMTA in ZnO nanowire growth. Langmuir 27:3672
43. Andeen D, Kim JH, Lange FF, Goh GKL, Tripathy S (2006) Lateral epitaxial overgrowth of ZnO in water at 90 degrees C. Adv Funct Mater 16:799
44. Pauporte T, Jouanno E, Pelle F, Viana B, Aschehoug P (2009) Key growth parameters for the electrodeposition of ZnO films with an intense UV-light emission at room temperature. J Phys Chem C 113:10422
45. Cui JB (2008) Defect control and its influence on the exciton emission of electrodeposited ZnO nanorods. J Phys Chem C 112:10385
46. Cui JB, Soo YC, Chen TP, Gibson UJ (2008) Low-temperature growth and characterization of Cl-doped ZnO nanowire arrays. J Phys Chem C 112:4475
47. Ren T, Baker HR, Poduska KM (2007) Optical absorption edge shifts in electrodeposited ZnO thin films. Thin Solid Films 515:7976
48. von Windheim JA, Wynands H, Cocivera M (1991) Removal and preparation of electrodeposited semiconductors for high impedance hall-effect measurements. J Electrochem Soc 138:3435
49. Guillemoles JF, Cowache P, Lusson A, Fezzaa K, Boisivon F, Videl J, Lincot D (1996) One step electrodeposition of $CuInSe_2$: improved structural, electronic, and photovoltaic properties by annealing under high selenium pressure. J Appl Phys 79:7293
50. Mizuno K, Izaki M, Murase K, Shinagawa T, Chigane M, Inaba M, Tasaka A, Awakura Y (2005) Structural and electrical characterizations of electrodeposited p-type semiconductor Cu_2O films. J Electrochem Soc 152:C179
51. Yoon S, Huh I, Lim JH, Yoo B (2012) Annealing effects on electrical and optical properties of ZnO thin films synthesized by the electrochemical method. Curr Appl Phys 12:784
52. Shinagawa T, Chigane M, Murase K, Izaki M (2012) Drastic change in electrical properties of electrodeposited ZnO: systematic study by hall effect measurements. J Phys Chem C 116:15925

53. Mora-Sero I, Fabregat-Santiago F, Denier B, Bisquert J, Tena-Zaera R, Elias J, Levy-Clement C (2006) Determination of carrier density of ZnO nanowires by electrochemical techniques. Appl Phys Lett 89:203117
54. Voss T, Bekeny C, Gutowski J, Tena-Zaera R, Elias J, Levy-Clement C, Mora-Sero I, Bisquert J (2009) Localized versus delocalized states: photoluminescence from electrochemically synthesized ZnO nanowires. J Appl Phys 106:054304
55. Samantilleke AP, Boyle MH, Young J, Dharmadasa IM (1998) Electrodeposition of n-type and p-type ZnSe thin films for applications in large area optoelectronic devices. J Mater Sci Mater Electron 9:289
56. Samantilleke AP, Boyle MH, Young J, Dharmadasa IM (1998) Growth of n-type and p-type ZnSe thin films using an electrochemical technique for applications in large area optoelectronic devices. J Mater Sci Mater Electron 9:231
57. Thomas MA, Cui JB (2010) Electrochemical route to p-type doping of ZnO nanowires. J Phys Chem Lett 1:1090
58. Wellings JS, Chaure NB, Heavens SN, Dharmadasa IM (2008) Growth and characterisation of electrodeposited ZnO thin films. Thin Solid Films 516:3893
59. Ahn KS, Deutsch T, Yan YF, Jiang CS, Perkins CL, Turner J, Al-Jassim MM (2007) Synthesis of band-gap-reduced p-type ZnO films by Cu incorporation. J Appl Phys 02:023517
60. Fan JD, Shavel A, Zamani R, Fabrega C, Rousset J, Haller S, Guell F, Carrete A, Andreu T, Arbiol J, Morante JR, Cabot A (2011) Control of the doping concentration, morphology and optoelectronic properties of vertically aligned chlorine-doped ZnO nanowires. Acta Mater 59:6790
61. Han XF, Han K, Tao M (2010) Electrodeposition of group-IIIA doped ZnO as a transparent conductive oxide. ECS Trans 15:93
62. Kemell M, Dartigues F, Ritala M, Leskela M (2003) Electrochemical preparation of In and Al doped ZnO thin films for $CuInSe_2$ solar cells. Thin Solid Films 434:20
63. Machado G, Guerra DN, Leinen D, Ramos-Barrado JR, Marotti RE, Dalchiele EA (2005) Indium doped zinc oxide thin films obtained by electrodeposition. Thin Solid Films 490:124
64. Ishizaki H, Imaizumi M, Matsuda S, Izaki M, Ito T (2002) Incorporation of boron in ZnO film from an aqueous solution containing zinc nitrate and dimethylamine-borane by electrochemical reaction. Thin Solid Films 411:65
65. Rousset J, Donsanti F, Genevee P, Renou G, Lincot D (2011) High efficiency cadmium free $Cu(In,Ga)Se_2$ thin film solar cells terminated by an electrodeposited front contact. Sol Energy Mater Sol Cells 95:1544
66. Han XF, Han K, Tao M (2010) Low resistivity yttrium-doped zinc oxide by electrochemical deposition. J Electrochem Soc 157:H593
67. Li GR, Zhao WX, Bu Q, Tong YX (2009) A novel electrochemical deposition route for the preparation of $Zn_{1-x}Cd_xO$ nanorods with controllable optical properties. Electrochem Commun 11:282
68. Lupan O, Pauporte T, Bahers TL, Ciofini I, Viana B (2011) High aspect ratio ternary $Zn_{1-x}Cd_xO$ nanowires by electrodeposition for light-emitting diode applications. J Phys Chem C 115:14548
69. Ishizaki H, Yamada N (2006) Preparation of $Zn_{1-x}Mg_xO$ film by electrochemical reaction. Electrochem Solid State Lett 9:C178
70. Li GR, Dawa CR, Lu XH, Yu XL, Tong YX (2009) Use of additives in the electrodeposition of nanostructured Eu_{3+}/ZnO films for photoluminescent devices. Langmuir 25:2378
71. Cui JB, Gibson UJ (2005) Electrodeposition and room temperature ferromagnetic anisotropy of Co and Ni-doped ZnO nanowire arrays. Appl Phys Lett 87
72. Cui JB, Zeng Q, Gibson UJ (2006) Synthesis and magnetic properties of Co-doped ZnO nanowires. J Appl Phys 99
73. Lipinski BB, Mosca DH, Mattoso N, Schreiner WH, de Oliveira AJA (2004) Electrodeposition of ZnO-Fe granular films. Electrochem Solid State Lett 7:C115
74. Li GR, Qu DL, Zhao WX, Tong YX (2007) Electrochemical deposition of (Mn, Co)-codoped ZnO nanorod arrays without any template. Electrochem Commun 9:1661

75. Thomas MA, Cui JB (2009) Investigations of acceptor related photoluminescence from electrodeposited Ag-doped ZnO. J Appl Phys 105:093533
76. Thomas MA, Sun WW, Cui JB (2012) Mechanism of Ag doping in ZnO nanowires by electrodeposition: experimental and theoretical insights. J Phys Chem C 116:6383
77. Briscoe J, Gallardo DE, Dunn S (2009) In situ antimony doping of solution-grown ZnO nanorods. Chem Commun 10:1273
78. Lupan O, Chow L, Ono LK, Cuenya BR, Chai GY, Khallaf H, Park SH, Schulte A (2010) Synthesis and characterization of Ag- or Sb-doped ZnO nanorods by a facile hydrothermal route. J Phys Chem C 114:12401
79. Tay CB, Chua SJ, Loh KP (2010) Stable p-type doping of ZnO film in aqueous solution at low temperatures. J Phys Chem C 114:9981
80. Fang X, Li JH, Zhao DX, Shen DZ, Li BH, Wang XH (2009) Phosphorus-doped p-type ZnO nanorods and ZnO nanorod p-n homojunction LED fabricated by hydrothermal method. J Phys Chem C 113:21208
81. Lee J, Cha S, Kim J, Nam H, Lee S, Ko W, Wang KL, Park J, Hong J (2011) p-type conduction characteristics of lithium-doped ZnO nanowires. Adv Mater 23:4183
82. Jin YX, Cui QL, Wang K, Hao JA, Wang QS, Zhang JA (2011) Investigation of photoluminescence in undoped and Ag-doped ZnO flowerlike nanocrystals. J Appl Phys 109:053521
83. Wang GP, Chu S, Zhan N, Zhou HM, Liu JL (2011) Synthesis and characterization of Ag-doped p-type ZnO nanowires. Appl Phys A Mater Sci Process 103:951
84. Fang F, Zhao DX, Fang X, Li JH, Wei ZP, Wang SZ, Wu JL, Wang XH (2011) Optical and electrical properties of individual p-type ZnO microbelts with Ag dopant. J Mater Chem 21:14979
85. Kang HS, Ahn BD, Kim JH, Kim GH, Lim SH, Chang HW, Lee SY (2006) Structural, electrical, and optical properties of p-type ZnO thin films with Ag dopant. Appl Phys Lett 88:202108
86. Chai J, Mendelsberg RJ, Reeves RJ, Kennedy J, von Wenckstern H, Schmidt M, Grundmann M, Doyle K, Myers TH, Durbin SM (2010) Identification of a deep acceptor level in ZnO due to silver doping. J Electron Mater 39:577
87. Thomas MA, Cui JB (2009) Electrochemical growth and characterization of Ag-doped ZnO nanostructures. J Vac Sci Technol B 27:1673
88. Kohan AF, Ceder G, Morgan D, Van de Walle CG (2000) First-principles study of native point defects in ZnO. Phys Rev B 61:15019
89. Zhang SB, Wei SH, Zunger A (2001) Intrinsic n-type versus p-type doping asymmetry and the defect physics of ZnO. Phys Rev B 63:075205
90. Yan YF, Al-Jassim MM, Wei SH (2006) Doping of ZnO by group-IB elements. Appl Phys Lett 89:181912
91. Volnianska O, Boguslawski P, Kaczkowski J, Jakubas P, Jezierski A, Kaminska E (2009) Theory of doping properties of Ag acceptors in ZnO. Phys Rev B 80:245212
92. Li YL, Zhao XA, Fan WL (2011) Structural, electronic, and optical properties of Ag-doped ZnO nanowires: first principles study. J Phys Chem C 115:3552
93. O'Regan B, Schwartz DT, Zakeeruddin SM, Gratzel M (2000) Electrodeposited nanocomposite n-p heterojunctions for solid-state dye-sensitized photovoltaics. Adv Mater 12:1263
94. Levy-Clement C, Tena-Zaera R, Ryan MA, Katty A, Hodes G (2005) CdSe-sensitized p- CuSCN/nanowire n-ZnO heterojunctions. Adv Mater 17:1512
95. Karuppuchamu S, Nonomura K, Yoshida T, Sugiura T, Minoura H (2002) Cathodic electrodeposition of oxide semiconductor thin films and their application to dye-sensitized solar cells. Solid State Ion 151:19
96. Lupan O, Pauporte T, Viana B (2010) Low-voltage UV-electroluminescence from ZnO-nanowire array/p-GaN light-emitting diodes. Adv Mater 22:3298
97. Cui JB, Gibson UJ (2007) Low-temperature fabrication of single-crystal ZnO nanopillar photonic bandgap structures. Nanotechnology 18:155302